Precision and Radiosonde Validation of Satellite Gridpoint Temperature Anomalies. Part II: A Tropospheric Retrieval and Trends during 1979–90

ROY W. SPENCER

Earth Science and Applications Division, NASA/Marshall Space Flight Center, Alabama

JOHN R. CHRISTY

Atmospheric Science Program, University of Alabama in Huntsville, Huntsville, Alabama

(Manuscript received 9 April 1991, in final form 20 November 1991)

ABSTRACT

TIROS-N satellite Microwave Sounding Unit (MSU) channel 2 data from different view angles across the MSU scan swath are combined to remove the influence of the lower stratosphere and much of the upper troposphere on the measured brightness temperatures. The retrieval provides a sharper averaging kernel than the raw channel 2 weighting function, with a peak lowered from 50 kPa to 70 kPa and with only slightly more surface influence than raw channel 2. Monthly 2.5° gridpoint anomalies of this tropospheric retrieval compared between simultaneously operating satellites indicate close agreement, 0.15°C in the tropics to around 0.30°C over much of the higher latitudes. The agreement is not as close as with raw channel 2 anomalies because synoptic-scale temperature gradient information across the 2000-km swath of the MSU is lost in the retrieval procedure and because the retrieval involves the magnification of a small difference between two large numbers. Single gridpoint monthly anomaly correlations between the satellite measurements and the radiosonde calculations range from around 0.95 at high latitudes to below 0.8 in the tropical west Pacific, with standard errors of estimate of 0.16°C at Guam to around 0.50°C at high-latitude continental stations. Calculation of radiosonde temperatures with a static weighting function instead of the radiative transfer equation degrades the standard errors by an average of less than 0.04°C. Of various standard tropospheric layers, the channel 2 retrieval anomalies correlate best with radiosonde 100–50- or 100–40-kPa-thickness anomalies. A comparison between global and hemispheric anomalies computed for raw channel 2 data versus the tropospheric retrieval show a correction in the 1979–90 time series for the volcano-induced stratospheric warming of 1982–83, which was independently observed by MSU channel 4. This correction leads to a slightly greater tropospheric warming trend in the 12-year time series (1979–90) for the tropospheric retrieval [0.039°C (±0.03°C) per decade] than for channel 2 alone [0.022°C (±0.02°C) per decade].

1. Introduction

In Part I of this study we showed the excellent agreement between separate *TIROS-N* satellites when independently measuring monthly anomalies of the Microwave Sounding Unit (MSU) channel 2 T_b at the 2.5° gridpoint level. The average gridpoint agreement between satellites was better than 0.07°C over the tropical oceans and usually better than 0.15°C elsewhere. When the satellite measurements were compared to radiosonde measurements of 10 years of monthly anomalies, good agreement was found with many correlations over 0.95 and standard errors of estimate of 0.15°C in the tropics to 0.25°C at high latitudes. In terms of conventionally measured atmospheric layers, the channel 2 anomalies correlated best with 100–15-kPa thickness anomalies. Decadal trends in both the satellite and radiosonde time series, as well as intercomparisons between satellites, showed no evidence for instrumental drift in MSU channel 2.

However, lower-stratospheric temperatures can behave differently than tropospheric temperatures, making the channel 2 overlap into these two regions a disadvantage for monitoring of tropospheric temperatures. Examination of 10-year radiosonde temperature trends for different layers of the atmosphere (Table 1) reveals that different regional trends can be experienced depending on the layer in question, even within the troposphere. Most of these regions, with the exception of the tropical Pacific, experienced considerably different trends above versus below the 30-kPa level. Note also that these 10-year trends are quite variable from region to region, making the lack of radiosonde data in remote regions a significant source of uncertainty in monitoring "global" temperature trends with radiosonde data. These differences suggest the need to remove as much of the upper troposphere and lower stratosphere as possible from the channel 2 measurements if maximum

Corresponding author address: Roy W. Spencer, ES43 Earth Science and Applications Division, NASA Marshall Space Flight Center, Alabama 35812.

TABLE 1. Composited radiosonde layer average temperature trends (°C) for the 10-yr period 1979–88 for different regions.

Layer (Kpa)	Florida[a]	U.S. northwest[b]	U.S. northeast[c]	Great Lakes[d]	Caribbean[e]	West Pacific[f]
30–15	−0.48	−1.28	−0.53	−0.92	−0.29	+0.14
50–30	−0.06	+1.34	+0.85	+1.14	−0.02	+0.10
70–50	−0.05	+1.37	+0.80	+1.31	+0.04	+0.07
85–70	0.00	+1.37	+0.84	+1.67	+0.19	+0.25

[a] Apalachicola, Tampa, Miami, Key West.
[b] Salem, Oregon; Quillayute, Washington.
[c] Caribou, Maine; Chatham, Massachusetts; Buffalo, New York; Albany, New York; Portland, Maine.
[d] Flint, Michigan; Peoria, Illinois; Green Bay, Wisconsin; International Falls, Minnesota; St. Cloud, Minnesota; Huron, South Dakota.
[e] Christ Church, Barbados; Santo Domingo, Dominican Republic; Piarco, Trinidad; San Juan, Puerto Rico; Curacao, Netherland Antilles.
[f] Yap Island; Koror Island; Ponape Island; Truk Island; Majuro Island; Guam; Wake Island.

utility of the satellite is to be made for monitoring a shallow layer that is expected to behave more uniformly (e.g., the lower and middle troposphere).

We can examine the global variability in the lower stratosphere during the period 1979–90 by applying the same procedures outlined in Part I of this study to MSU channel 4 (Fig. 1). All intersatellite statistics on monthly agreement and long-term stability of MSU channel 4 (not shown) are even better than those reported for channel 2 in Part I, making channel 4 a superb resource for monitoring global lower-stratospheric temperature trends. When we compute the channel 4 temperature anomalies for the period 1979–90 (Fig. 2) we find a strong warm event during 1982–83. This appears to be superimposed upon an average cooling trend, although this cooling appears to have leveled off since 1985. The 1982–83 warming is generally attributed to infrared absorption by sulfuric acid aerosols formed from sulfur dioxide injected into the stratosphere by El Chichón volcano in early 1982 and by Nyamuragria volcano in December 1981. This warm event happened to occur during the tropospheric El Niño–Southern Oscillation (ENSO) warm event as seen by MSU channel 2 (also in Fig. 2). Since MSU channel 2 was viewing the tropospheric ENSO warmth "through" the stratospheric warmth, to the extent that the MSU channel 2 and 4 weighting functions in Fig. 1 overlap, the channel 2 warming might be partially due to the stratospheric event. Correction for any stratospheric influence would be even more important at high latitudes where the base of the stratosphere is much lower than in the tropics.

Fortunately, it is possible to combine MSU channel 2 data from various view angles in such a way as to cancel out the stratospheric contribution and achieve a vertical weighting distribution that is sharper than what a single channel can offer. Here we describe a method for removing most of the stratospheric influ-

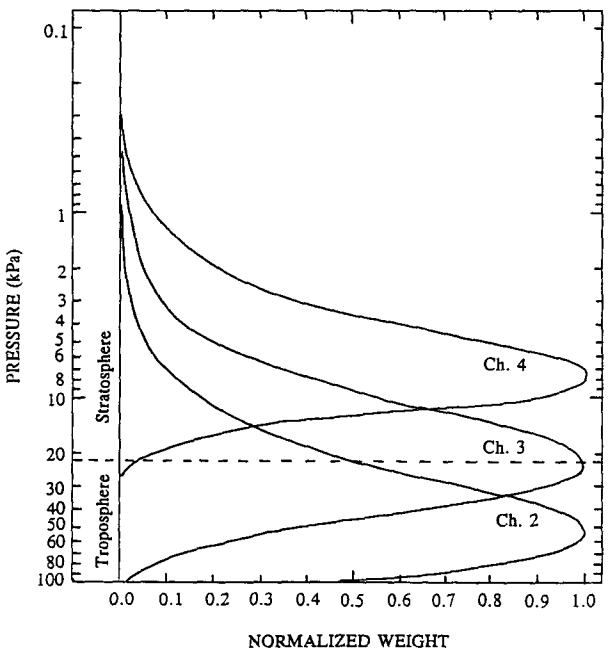

FIG. 1. MSU channel 2, 3, and 4 weighting functions for a nadir view through a *U.S. Standard Atmosphere.*

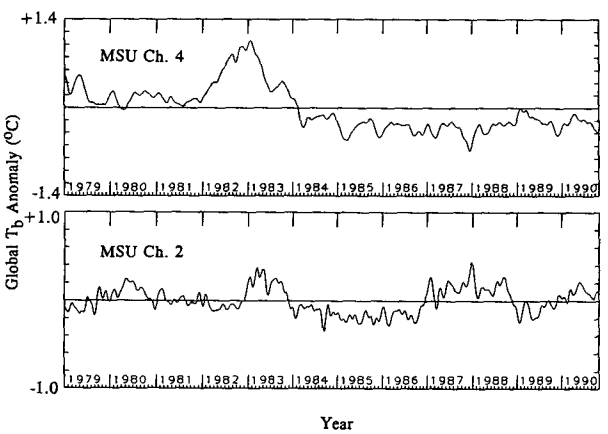

FIG. 2. MSU channel 4 (stratosphere) and channel 2 (troposphere) temperature anomalies during 1979–90, assembled by the method described in the Appendix of Part I. Anomalies have been low-pass filtered, with a half-power point at 40 days.

ence on channel 2 based on the differencing of MSU channel 2 near-nadir and limb measurements through the "averaging kernel" concept. This concept was originally described in the context of atmospheric temperature retrievals by Conrath (1972), where weighting functions can be linearly combined to achieve different vertical distributions of weighting. This is the fundamental basis for any satellite temperature retrieval procedures and is in effect a deconvolution of overlapping weighting functions. This technique was discussed more recently by Grody (1980). Also, updated tropospheric time series of both channel 2 and the tropospheric retrieval are presented for the period 1979–90.

2. Multiangle retrievals of deep-layer temperature

a. Retrieval philosophy

Retrieval of temperature information from the MSU (or other satellite sounding radiometers) is usually performed for specific pressure levels through various retrieval procedures that in effect deconvolve overlapping weighting functions into a sharper averaging kernel. The retrieval of specific pressure level information has provided conformity with traditional radiosonde measurements and with numerical weather prediction models that have been tailored to accept radiosonde data. Unfortunately (as discussed in Part I), even though deconvolution of these weighting functions can achieve an averaging kernel that is sharper than the original weighting functions, it is not possible to reduce the depth of the deconvolved layer beyond certain limits imposed by the finite number of channels and the existence of noise in those channels. Thus, a satellite-based retrieval for a specific pressure level will always use information representative of a deep atmospheric layer. Any attempts to retrieve a temperature for a specific pressure level must use ancillary information, usually with radiosondes.

Because we wish to determine the utility of satellites for temperature monitoring, we restrict ourselves (by necessity) to temperatures averaged over deep layers. For climate monitoring this is not necessarily bad. The individual channel weighting functions can in principle be used by themselves (as we saw in Part I), provided that their vertical weighting distribution is considered useful.

Removal of the stratospheric influence on MSU channel 2 might be accomplished through some deconvolution from MSU channel 3, which has information from the layer whose influence we wish to remove (Fig. 1). Unfortunately, our analysis of 12 years (1979–90) of MSU channel 3 data reveals that one or more MSUs show some sizeable calibration drifts in channel 3, evidenced by a trend in their difference (Fig. 3). While this drift is actually the difference in drifts between the two sensors, we have seen evidence to suggest that it is the *NOAA-6* channel 3 that is drifting, which over the period represented in Fig. 3 would amount to 0.3°C. [The step function character of the drift in channel 3 is a result of the removal of a 1-year annual cycle (1982) that was not detrended. The drift by itself seems to be linear in time.] This amount of instrumental drift, if left uncorrected, is too large to accept for climate monitoring purposes. Channel 3 drift problems were found for at least one other satellite, probably *NOAA-9,* for which the drift is much more erratic. As a consequence of these drift problems, use of MSU channel 3 for any type of long-term climate monitoring should be done with extreme caution.

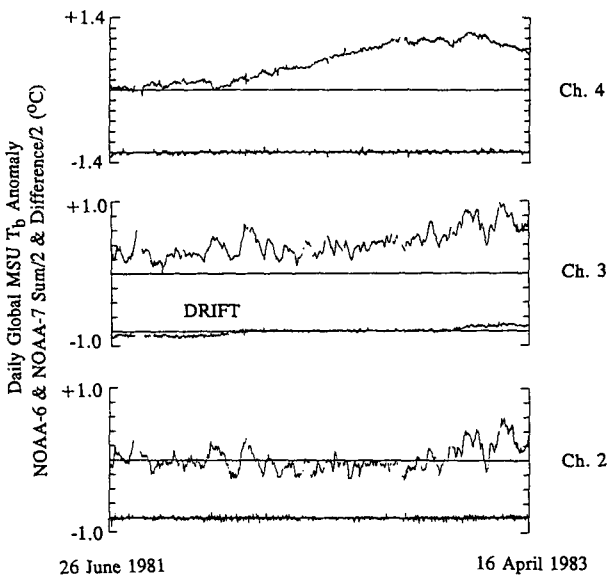

FIG. 3. Time series of globally averaged *NOAA-6* and *NOAA-7* sums (widely varying line) and differences (slightly varying line) of daily MSU channels 2, 3, and 4 T_b anomalies. Drift in channel 3 is evident in the difference time series.

b. The tropospheric retrieval and its global precision

Fortunately, it turns out that if the goal is the removal of the stratospheric influence on MSU channel 2, then a linear combination of channel 2 data from different view angles [channel "2R", Eq. (1)] provides better stratospheric canceling than any combination of channels 2 and 3.

$$\text{channel 2R } T_b = 4[T_{b3} + T_{b4} + T_{b8} + T_{b9}]/4 - 3[T_{b1} + T_{b2} + T_{b10} + T_{b11}]/4. \quad (1)$$

This is shown in Fig. 4 where the view angles corresponding to MSU scan positions (1, 2, 10, 11) and (3, 4, 8, 9) can be combined with appropriate weighting to yield a new weighting function that removes most of the stratospheric influence, lowers and sharpens the peak of the averaging kernel, and results in only slightly more sensitivity to the surface than even the channel

2 nadir scan position (6) provides. (SCG addressed the contaminating nonthermometric influence of surface changes on MSU channel 2). The use of eight scan positions was chosen to minimize measurement retrieval noise, which is greater than raw channel 2 noise because the retrieval involves the magnification of small differences between two large numbers. For our simple linear retrieval, after a ratio of weights is chosen that provides stratospheric canceling of the individual scan angle weighting functions in Fig. 4, the weights can then be adjusted so that their sum equals 1 [Eq. (1)]. This results in the retrieval being an accurate brightness temperature for the averaging kernel distribution of weighting. The small amount of negative area under the channel 2R averaging kernel in Fig. 4, although probably insignificant in comparison to uncertainties in the oxygen absorption theory, would lead to a miniscule warming in the channel 2R T_b if stratospheric cooling occurs, and vice versa. Separate retrievals for the two halves of the scan swath were attempted but showed poor agreement between simultaneously operating satellites' monthly anomalies.

Because computation of channel 2R requires a full swath width of data, horizontal temperature gradients across the 2000-km wide MSU swath are lost. This gradient information had been retained in our channel 2 study (Part I) through the limb correction procedure. Thus, we cannot expect channel 2R to provide very useful synoptic-scale temperature information on short time scales. It should, however, provide useful zonal, hemispheric, and global averages since the temperature gradient errors should average out in a zonal average. Also, because the retrieval magnifies the difference between two large numbers [Eq. (1)], any errors in the measured T_b also get magnified by the same amount.

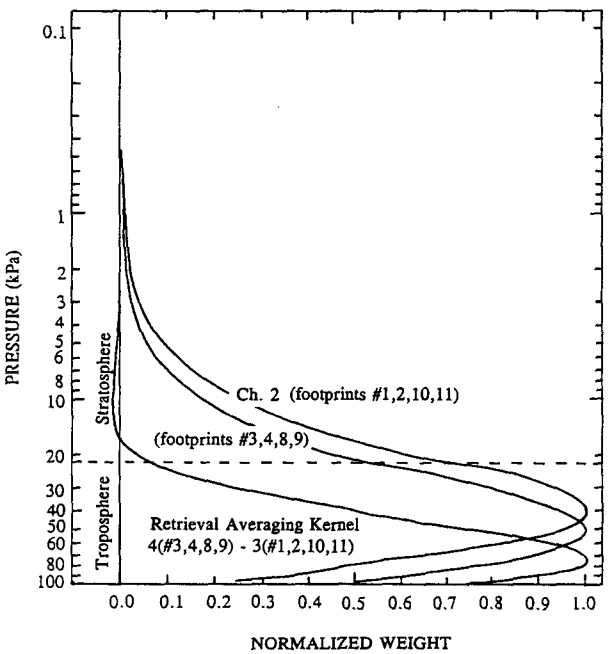

FIG. 4. Scan-angle–averaged MSU channel 2 weighting functions for scan positions 1, 2, 10, 11 and 3, 4, 8, 9 and a retrieval averaging kernel (channel 2R) computed through a linear combination of functions of the other two weighting functions.

The same procedures for gridpoint assignment, satellite intercalibration, and anomaly calculation at both the 2.5° gridpoint and zonal levels were used as described for raw channel 2 data in Part I. However, since the full swath of data is required for the retrieval, no limb corrections are applied to the individual MSU scan positions. The channel 2R T_b were assigned to only the middle three MSU scan position locations. From this point onward all daily gridpoint assignment and interpolation to empty grid squares, monthly averaging, satellite intercalibration, and annual cycle removal follow the same procedures as were described in Part I for channel 2.

As in Part I for channel 2 anomalies, we present the single-satellite gridpoint channel 2R T_b standard deviation field (Fig. 5a) and signal-to-noise field (Fig. 5b) computed from a 20-month overlap period of *NOAA-6* and *NOAA-7*. We see from Fig. 5a that the deep tropics have a single-satellite error of less than 0.15°C and higher latitudes generally less than 0.3°C. Scattered high-latitude land areas show errors of 0.45°C with isolated embedded values of 0.6°. These are poorer than those values shown for channel 2 in Part I and lead us to expect somewhat poorer gridpoint agreement with the radiosonde calculations (below) than was found with raw channel 2. Nevertheless, the corresponding signal-to-noise (S/N) distribution (Fig. 5b) indicates that most of the earth has S/N ratio over 25 with some small areas dropping below 10. Although not as good as the S/N ratio for raw channel 2 in Part I, these are still sufficiently high to make the channel 2R gridpoint dataset useful for many purposes.

As expected, global averaging of the anomalies further improves the satellite agreement (Table 2). It can be seen through comparison of this table with Table A1 of Part I that the monthly global signal-to-noise ratio is not as good for the tropospheric retrieval anomalies as it is for raw channel 2 anomalies. The standard deviation of the difference between satellites for single-satellite monthly global anomalies is often closer to 0.02°C compared to 0.01°C for channel 2 anomalies. This is, however, sufficiently good for the multimonth overlap periods to allow accurate intercalibration between satellites for long-term monitoring on a global or hemispheric basis.

3. Radiosonde comparisons to Channel 2R

a. Single station

The monthly gridpoint channel 2R anomalies were compared to radiosonde data with the same three methods used for the channel 2 anomalies in Part I.

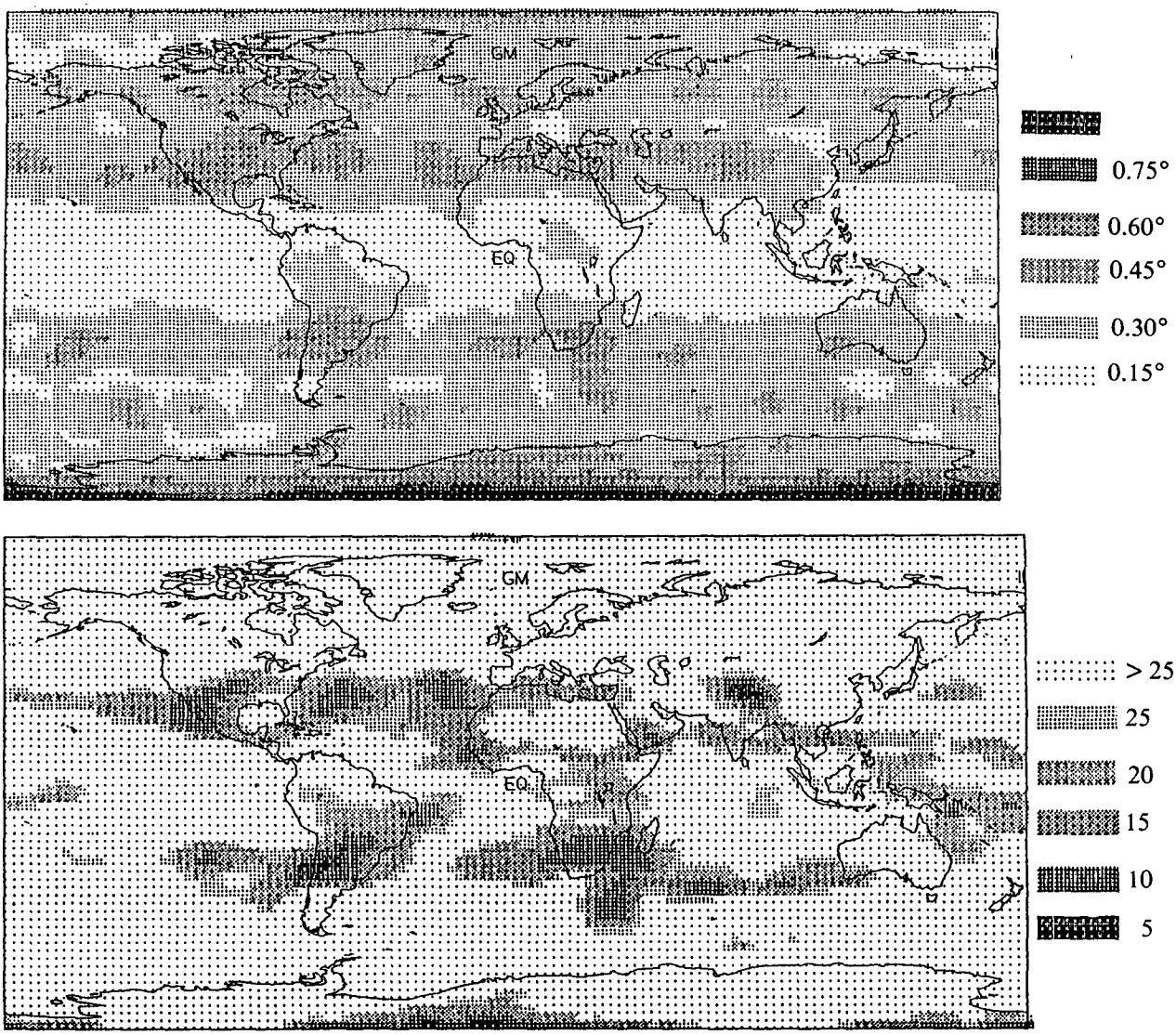

FIG. 5. Single-satellite gridpoint channel 2R T_b anomaly error estimates (top) and signal-to-noise ratios (bottom) computed from the levels of monthly agreement between *NOAA-6* and *NOAA-7* during a 20-month overlap period.

These include radiosonde computations of channel 2R T_b with 1) the radiative transfer equation, 2) a constant (standard atmosphere) weighting profile (Fig. 4) in combination with Eq. (2) from Part I, and 3) comparisons to standard pressure level thicknesses. As in Part I, we computed thickness anomalies for all com-

TABLE 2. Global 1-day and 30-day statistics of all overlaps between MSUs for the channel 2 tropospheric temperature retrieval anomalies.

Satellite route to *NOAA-6*	Overlap dates	Number of days	Daily error (2 sat.)	Daily S/N	30-day error (2 sat.)	30-day S/N
TIROS-N to *NOAA-6*	1 Jul 1979–19 Jan 1980	156	.066°	7	.017°	20
NOAA-6 Base						
NOAA-7 to *NOAA-6*	26 Jun 1981–16 Apr 1983	566	.061°	8	.011°	124
NOAA-9 to *NOAA-6*	30 Oct 1985–4 Nov 1986	228	.061°	18	.011°	74
NOAA-10–NOAA-9	26 Nov 1986–7 Mar 1987	96	.065°	12	.009°	300
NOAA-11–NOAA-10	23 Oct 1988–31 Dec 1990	678	.062°	8	.020°	40

binations of layers having bases at either 100 or 85 kPa and tops ranging from 70 to 10 kPa. Also consistent with Part I, we present comparisons between channel 2R and the radiosonde channel 2R and thickness temperature anomalies at Cold Bay, Alaska (Fig. 6); St. Cloud, Minnesota (Fig. 7); Oakland, California (Fig. 8); Lihue, Hawaii (Fig. 9); San Juan, Puerto Rico (Fig. 10); and Guam (Fig. 11).

At Cold Bay (Fig. 6), we find a monthly correlation of .94 and SE = 0.50°C between the MSU measured anomalies and the radiosonde anomalies calculated with the radiative transfer equation. When the static weighting method is applied to the radiosonde temperature profile, the SE degrades by only 0.02°C to 0.52°C. When compared to the standard layers measured by radiosondes, the layers starting at 100 kPa, rather than 85 kPa, had the best correlations with the MSU. This is to be expected from the weighting profile shown in Fig. 4. For Cold Bay, as well as all other stations, we find that the best correlations to the retrieval exist with either the 100–50 or 100–40-kPa layers.

At St. Cloud, Minnesota (Fig. 7), R = .97 and SE = 0.48°C, results are similar to Cold Bay, Alaska. The static weighting method resulted in only 0.01°C degradation in the standard error. The 100–40-kPa layer had the best correlation of all conventionally measured radiosonde layers, with R = 0.95 and SE = 0.54°C.

At Oakland, California (Fig. 8), R = .91 and SE = 0.54°C. Use of the static weighting function method leads to SE = 0.58°C. The highest correlation with a standard layer is the 100–50-kPa layer with R = .91 and SE = 0.70°C.

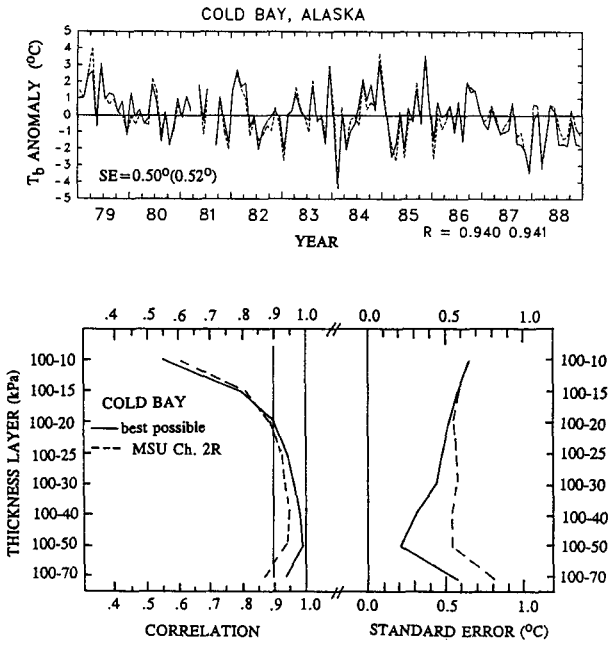

FIG. 6. Time series (a) of MSU channel 2R anomalies and radiosonde-calculated channel 2R anomalies, and correlations and standard errors (b) with radiosonde thickness temperature anomalies for Cold Bay, Alaska, during 1979–88. In (a) the solid line is MSU measured, the dashed line is radiosonde measured, and the correlations (R) are for the monthly and yearly anomalies, respectively. In (b) the solid line shows the best agreement possible based upon MSU channel 2R T_b being computed from the radiosonde data, and the dashed line shows the satellite-measured agreement with the radiosonde thickness temperature anomalies.

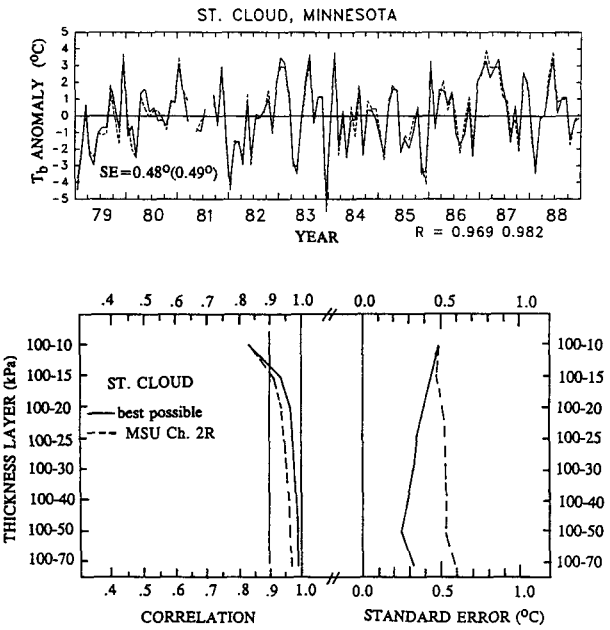

FIG. 7. As in Fig. 6 except St. Cloud, Minnesota.

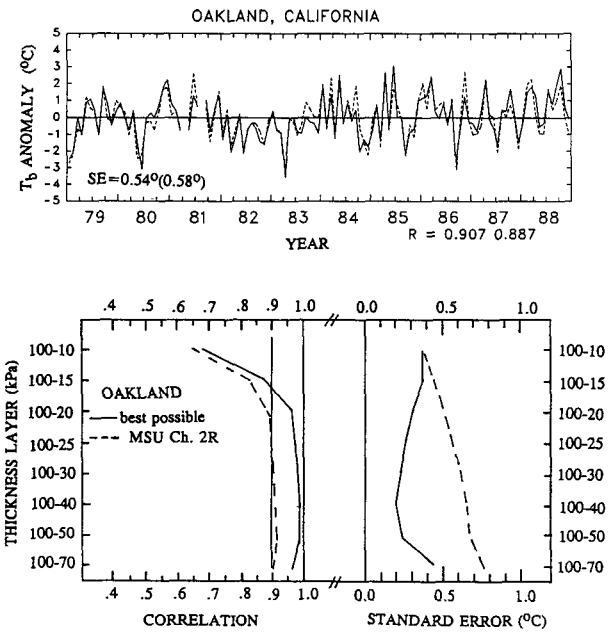

FIG. 8. As in Fig. 6 except Oakland, California.

In Lihue, Hawaii (Fig. 9), R = 0.89 and SE = 0.25°C. Use of the static weighting function yields SE = 0.32°C. The highest correlation with a standard radiosonde layer is 0.88, with SE = 0.31°C.

At San Juan, Puerto Rico (Fig. 10), R = .84 and SE = 0.29°C. Slight degradation to SE = 0.33°C is seen when the standard atmosphere weighting function is applied to the radiosonde temperature profile. Correlation to the 100–40-kPa thickness anomalies is also .84, with SE = 0.35°C.

The worst correlations are seen for Guam (Fig. 11), R = .74, but as was the case for the channel 2 comparisons, this is because the monthly anomaly signal is so small that it approaches the noise of the radiosonde and satellite systems. In fact, the correlation with the satellite is about the same as between adjacent tropical radiosonde stations for the 100–40-kPa layer (0.76), while the standard error of estimate the satellite provides (0.16°C) is near the limit of the radiosondes ability to measure monthly anomalies anyway, as discussed in Part I. It is also consistent with the tropical single satellite error of around 0.15°C shown in Fig. 5. Use of the static weighting function method gives SE = 0.20°C. The layer of highest correlation is 100–40 kPa, with R = 0.66 and SE = 0.21°C.

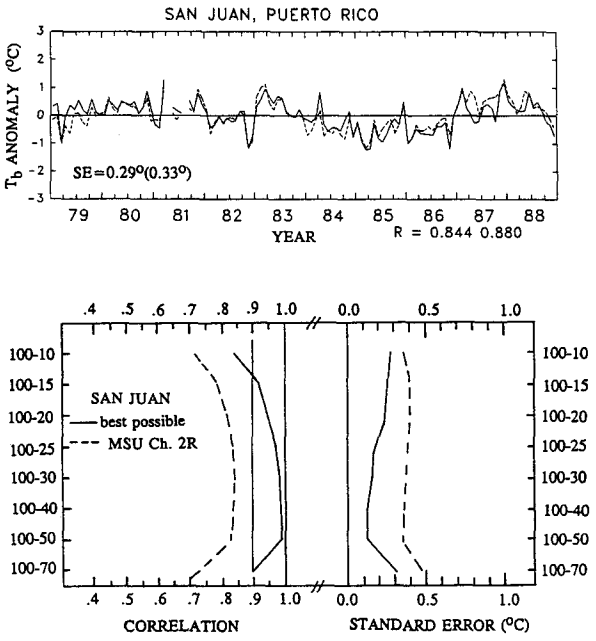

FIG. 10. As in Fig. 6 except San Juan, Puerto Rico.

b. *Composite stations*

As was done for channel 2 in Part I, we computed statistics for radiosonde station groupings from several regions (Table 3). We find that these station groupings improve the levels of agreement considerably, with standard errors ranging from 0.11° over the tropical west Pacific to around 0.35°C at high latitudes and correlations sometimes exceeding 0.95 at high latitudes. These results suggest that regionally averaged channel 2R anomalies have a smaller error than the individual gridpoint anomalies have (recall from Table 2 that the globally averaged single-satellite monthly error is about 0.02°C).

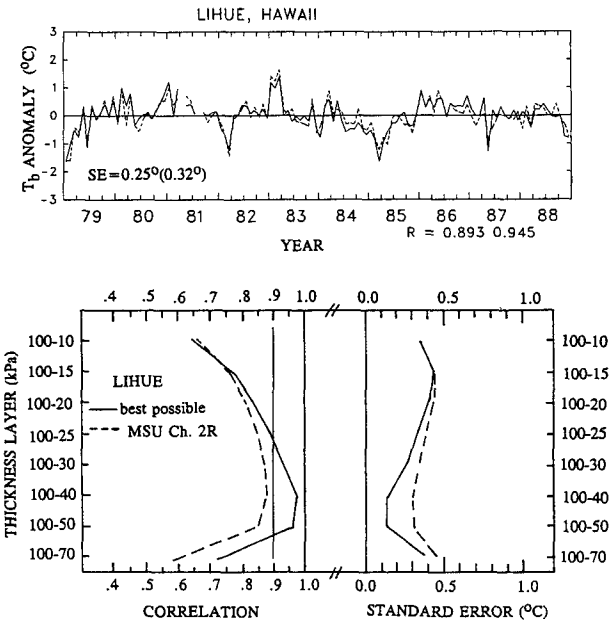

FIG. 9. As in Fig. 6 except Lihue, Hawaii.

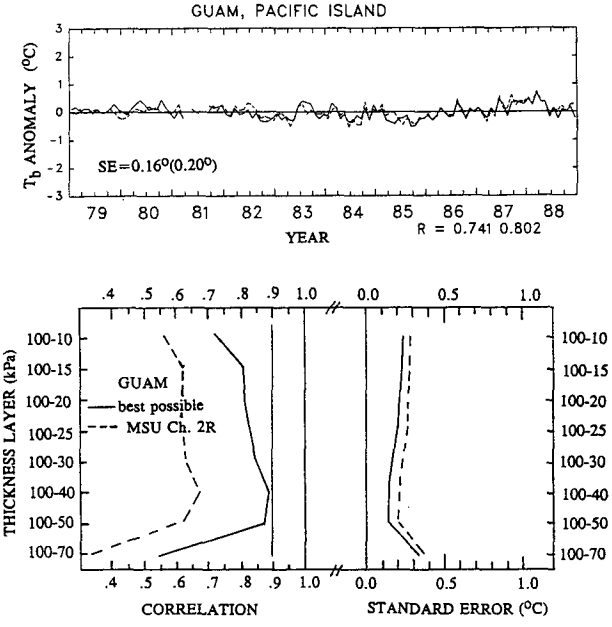

FIG. 11. As in Fig. 6 except Guam.

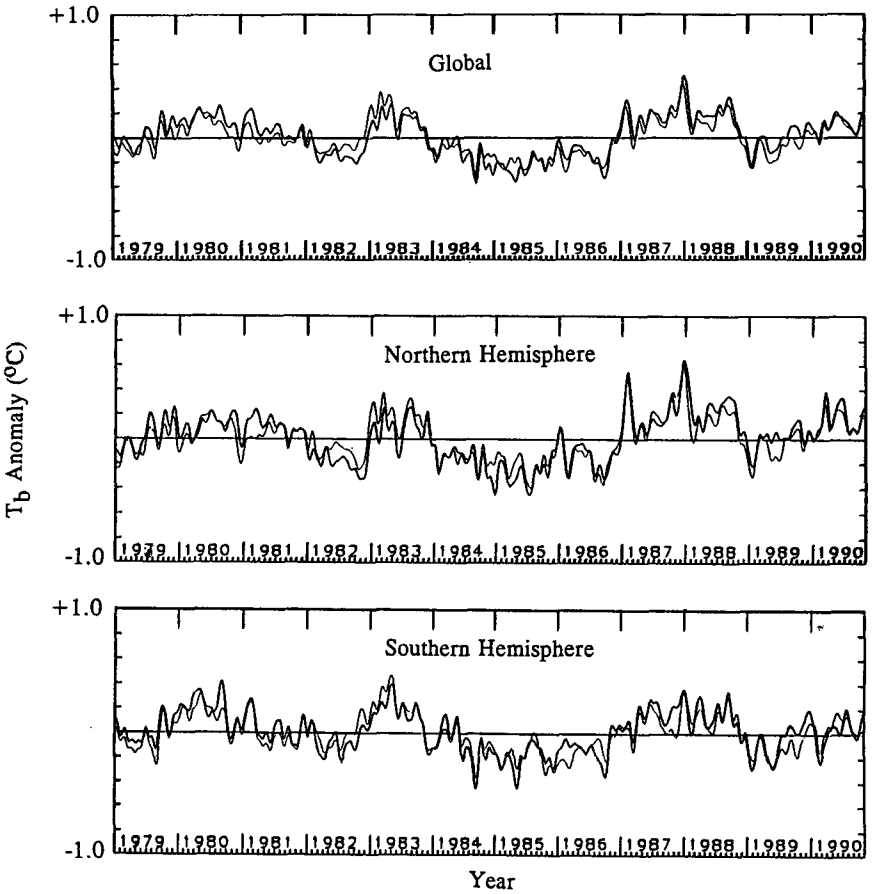

FIG. 12. MSU channel 2 (thin line) and tropospheric retrieval (thick line) T_b time series for the globe, Northern Hemisphere, and Southern Hemisphere during 1979–90. Series have been low-pass filtered with a filter half-power point at 40 days.

4. Retrieved tropospheric trends 1979–90

The good large-scale quality of the channel 2R gridpoint anomalies, combined with the small (0.02°C) monthly disagreement between simultaneously operating satellites (Table 1), suggests that hemispheric and global temperature trends in the lower half of the troposphere can be monitored with this retrieval. The tropospheric retrieval temperature anomalies for 1979–90 are shown in Fig. 12 superimposed on the channel 2 anomalies. The largest difference between channels 2 and 2R is seen in 1982–83, where the stratospheric warm event's influence has now been removed. Other differences can also be seen throughout the time series that, since apparently not stratospheric adjustments (they have no corresponding stratospheric anomaly in Fig. 2), probably indicate variations in globally averaged tropospheric stability. That most of these differences between channel 2 and 2R are real is supported by their large magnitude (0.1°C–0.2°C) relative to the monthly level of channel 2R disagreement between simultaneously operating satellites in Table 1 (0.01° to 0.02°C).

Of some importance is the finding that the decadal trend of the data is somewhat warmer for channel 2R (+0.039°C) than it is for the raw channel 2 time series (+0.015°C). The removal of the stratospheric influence on MSU channel 2 during 1982–83 is probably the major reason for the difference in long-term trends between channel 2 and 2R since it occurred in the first half of the 12-year record. The channel 2R trend is a combination of a Northern Hemisphere trend of +0.094°C and a Southern Hemisphere trend of −0.016°C. Because of the lack of any absolute truth, error bars on these trends are difficult to establish. However, because of the combined influence of small errors in our ability to intercalibrate satellites (0.01°) and our inability to discern instrumental drift to better than 0.01°, we estimate that the decadal trends are probably accurate to ±0.03°C for channel 2R and ±0.02°C for channel 2. This would make the decadal trends for 1979–90 not significantly different from zero.

TABLE 3. Station composite correlations and standard errors of satellite versus radiosonde monthly anomalies in channel 2R. Numbers in parentheses are the corresponding single-station values from the stations represented in Figs. 5–10.

Region	R	SE
Alaska (15)	.97 (.94)	.31° (.50°)
Great Lakes (6)	.98 (.97)	.37° (.48°)
West Coast (4)	.95 (.91)	.35° (.54°)
Caribbean (6)	.91 (.84)	.16° (.29°)
West Pacific (7)	.83 (.74)	.11° (.16°)

Alaska (15): Anette, Yakutat, Kodiak, King Salmon, Cold Bay, Adak, St. Paul Island, Anchorage, Fairbanks, McGrath, Bethel, Kotzebue, Nome, Barter Island, Barrow. Great Lakes (6): Sault Ste. Marie, MI; International Falls, MN; Green Bay, WI; St. Cloud, MN, Huron, SD. U.S. West Coast (4): Quillayute, WA; Salem, OR; Oakland, CA; San Diego, CA. Tropical West Pacific (7): Koror, Yap, Majuro, Wake, Guam, Truk, Ponape. Caribbean (6): Christ Church, Barbados; Santo Domingo, Dominican Republic; Piarco, Trinidad; San Juan, Puerto Rico; Curacao, Netherland Antilles; Roberts, Cayman Islands.

5. Conclusions

A procedure for removal of the stratospheric influence on MSU channel 2 for more useful long-term tropospheric temperature monitoring has been applied to MSU channel 2 data from 1979 to 1990 and was tested with radiosonde data during 1979–88. Intersatellite comparisons reveal single-satellite gridpoint errors of 0.15°C in the tropics to around 0.3°C over much of the higher latitudes. Scattered locations (including the United States) have errors of 0.6°C. Single gridpoint comparisons with individual radiosonde stations give correlations ranging from 0.97 (SE = 0.48°C) at St. Cloud, Minnesota, where the monthly tropospheric temperature anomaly signal is strong, to 0.74 (SE = 0.16°C) at Guam where the signal is very weak compared to the limiting accuracy of both the radiosonde and satellite systems. Groupings of stations improve the standard errors to 0.11°C over the west Pacific to SE = 0.35°C at high latitudes, with correlations ranging from 0.83 to 0.98, respectively. As was the case for the channel 2 results in Part I, the tropical standard errors reach the levels of agreement displayed by adjacent radiosonde stations. Best agreement with standard layers that radiosondes traditionally measure is with either 100–50 or 100–40-kPa layer anomalies.

For tropospheric temperature trends, the tropospheric retrieval shows some differences with raw channel 2 data, particularly during 1982–83 when stratospheric warming exaggerated the MSU channel 2 warm signal of the 1982–83 ENSO event. Other differences between channel 2 and 2R variations are probably related to variations in tropospheric stability. The satellite record trends for the retrieval differ from the channel 2 trends by only 0.01°C, with a tropospheric retrieval trend of 0.039°C [±0.03°C] per decade and a channel 2 trend of 0.022°C [±0.02°C] per decade for the period 1979–90.

Acknowledgments. We thank Norman Grody (NOAA/NESDIS) for helpful advice during this study. This research was supported by the NASA Climate and Hydrologic System program.

REFERENCES

Conrath, B. J., 1972: Vertical resolution of temperature profiles obtained from remote radiation measurements. *J. Atmos. Sci.*, **29**, 1262–1271.

Grody, N. C., 1980: Analysis of satellite-based microwave retrievals of temperature and thermal winds: Effects of channel selection and a-priori mean on retrieval accuracy. *Remote Sensing of the Atmosphere and Oceans*, A. Deepak, Ed., Academic Press, 381–410.

Spencer, R. W., and J. R. Christy, 1990: Precise monitoring of global temperature trends from satellites. *Science*, **247**, 1558–1562.

——, ——, and N. C. Grody, 1990: Global atmospheric temperature monitoring with satellite microwave measurements: Method and results, 1979–84. *J. Climate.*, **3**, 1111–1128.